Altered Muscle Networks in Post-Stroke Survivors

by
Michael James Houston

A thesis submitted to the Department of Biomedical Engineering,
Cullen College of Engineering
in partial fulfillment of the requirements for the degree of

MASTER OF SCIENCES

in Biomedical Engineering

Chair of Committee: Yingchun Zhang, PhD

Committee Member: Jinsook Roh, PhD

Committee Member: Xiaoyan Li, PhD

University of Houston
December 2020

DEDICATION

I would like to dedicate this work to my parents as they have always supported me and my academic career every step of the way. I would not be where I am now without them, and God's help.

ACKNOWLEDGMENTS

ABSTRACT

Introduction

Functional interactions among muscles, indicated by muscle networks, reflect the effort of the central nervous system in reducing the redundancy of the musculoskeletal system in motor control. Efforts have been devoted to characterizing muscle network patterns in healthy subjects, however, alterations of muscle networks associated with stroke remain unexplored.

Methods

Muscle networks were assessed for eight key upper extremity muscles in mild, moderate, and severe stroke survivors and compared to healthy controls to identify stroke linked alterations in the neural oscillatory drive to muscles. Intermuscular coherence was computed for all possible muscle connections and were further decomposed via non-negative matrix factorization (NNMF) to identify the common spectral patterns of coherence underlying the muscle networks.

Results

Results demonstrated that the number of identified muscle networks during force generation is reduced in stroke survivors compared to healthy controls, and the number decreases as the severity of stroke increases. Stroke patients also showed reduced coherence of higher frequencies, particularly in the in the alpha, beta, and gamma bands.

Conclusions

The findings in this study could provide a new prospective for understanding the motor control recovery during post-stroke rehabilitation and inform future motor rehabilitation for post-stroke survivors.

TABLE OF CONTENTS

LIST OF TABLES

LIST OF FIGURES

CHAPTER 1 – INTRODUCTION

1.1 Background

The central nervous system (CNS) simplifies motor-control tasks by simultaneously co-activating sets of muscles as motor modules to reduce the high degrees of freedom of the musculoskeletal system (Bizzi et al., 1991; Bizzi et al., 2008). Muscle synergies are defined as sets of muscles typically activated together as motor modules during force generation (Davella et al., 2003; Bizzi and Cheung, 2013), and can be calculated using non-negative matrix factorization (NNMF) to identify anatomical coordination of muscles (Lee and Seung, 1999). However, muscle synergies cannot quantify the functional synchrony among muscles as intermuscular coherence can (Li et al., 2016). Coherence is a measure of associativity between two signals at certain frequencies, and intermuscular coherence can be used to assess the common neural input among muscles.

Stroke is a debilitating motor-impairment disease that severely affects motor control and muscle coordination, leading to abnormal patterns in force generation in affected muscles. The effects of stroke on motor-task performance have traditionally been studied via muscle synergy analysis (Roh et al., 2013; Roh et al., 2015) as well as intermuscular coherence (Kisiel-Sajewicz et al., 2011; Fisher et al., 2012). In 2013 *Roh et al.* discovered alterations in muscle synergy patterns in chronic severe stroke patients which were not observed in healthy controls. Abnormal co-activation of the anterior, middle, and posterior deltoid fibers was identified in the severely impaired stroke patients whereas healthy controls exhibited co-activation of the anterior and

middle deltoids in one synergy and co-activation of the middle and posterior deltoids in another synergy. The clavicular fibers of the pectoralis major were also discovered to become more isolated in a separate muscle synergy in severe stroke patients whereas the pectoralis major was synergistic with the anterior and middle deltoid fibers in healthy controls. *Roh et al.* furthered these results in 2015 by including mildly and moderately impaired stroke patients in the study. It was found that alterations to proximal muscle synergies were evident in lesser severity of stroke impairment, but still most pronounced in the severe stroke patients. Synergies relevant to shoulder movement were most affected in the lesser severity stroke patients, potentially indicating an inability for post-stroke survivors to selectively activate deltoid muscles. *Kisiel-Sajewicz et al*. discovered reduced functional coupling between the synergistic muscle pair of anterior deltoid and triceps brachii muscles in a target reaching paradigm using intermuscular coherence when comparing severe stroke impairment to healthy controls in the frequency range of $0 - 11$ Hz. These results suggested that reduced functional connectivity between synergistic muscles can help explain poor motor control in target-reaching tasks and could be due to the loss or reduction of the common oscillatory neural drive as input to muscles at the specified frequency range, likely as a result of damage to the cortico-spinal pathways. *Fisher et al.* concluded from their study that intermuscular coherence in the beta band ($15 - 30$ Hz) was dependent on the presence of an intact cortico-spinal tract, despite possible anterior horn cell destruction. Beta band intermuscular coherence was observed to be greater in magnitude for healthy controls versus patients with primary lateral sclerosis

and was shown to have great promise in acting as a sub-clinical biomarker for motor neuron disease.

Additional studies have also identified modulations to the neural drive to muscles in functional connectivity studies using coherence. In one study involving hand muscles in two distinct pinch tasks, modulations to the oscillatory neural drive were found as either an increase or decrease in coherence at the 10 Hz and 40 Hz (Laine and Valero-Cuevas 2017). The presence of somatosensory feedback in bimanual upper arm flexion and extension was also found to increase the neural coupling between muscles in the alpha and gamma bands (Nguyen et al., 2017). Task-dependent modulations of intermuscular coherence in the 15 – 30 Hz range was also discovered during a ramping force generation versus force hold period study (Kilner et al., 1999). Coherence has also been studied between the brain and muscles using MEG recordings (Kilner et al., 2000). *Kilner et al.* reported beta band coherence in the 15 – 30 Hz range to be related to specific parameters of hand motor function based on their experimental design based on precision grip tasks.

1.2 Contribution to The Field

Muscle network analysis is a novel method which was recently developed to study the functional connectivity of muscles in order to further explain the neural origin of muscle synergies and their capacity to simplify motor control (Boonstra et al., 2015). So far, coherence muscle networks have only been studied in healthy individuals during postural tasks (Boonstra et al., 2015; Kerkman et al., 2018) as well as gait analysis (Kerkman et al., 2020). While muscle synergies and intermuscular coherence

have been studied separately in stroke patients they have not been studied together. It has been shown by *Boonstra et al.* and *Kerkman et al.* that muscle synergies and coherence muscle networks are complementary to each other and both necessary in order to explain the effort of the central nervous system in simplifying motor control and the vast number of degrees of freedom in the musculoskeletal system. There is a clear lack of information regarding functional muscle connectivity in terms of coherence muscle networks in the stroke disease group which can help better understand the changes in muscle synergies as stroke impairment increases in severity. In this study, functional muscle connectivity is explored from isometric force generation of post-stroke survivors of various impairment levels and compared to functional connectivity of healthy controls through intermuscular coherence and muscle network analysis.

1.3 Hypothesis and Specific Aims

This study aims to provide a detail-oriented perspective into the negative effects stroke can have on functional muscle connectivity via muscle network analysis. Three specific aims are proposed in order to test this hypothesis. Considering the previous background information, it is hypothesized that stroke induces some alterations to the functional connectivity among muscles which are manifest in the muscle networks. The first specific aim entails analyzing the power spectral density (PSD) of upper-arm muscles during isometric force generation to observe any primary underlying differences in the frequency domain which will ultimately results in some intergroup differences of intermuscular coherence. The second specific aim involves calculating

the intermuscular coherence (IMC) of muscle pairs for mild, moderate, and severe post-stroke survivors and statistically comparing them to intermuscular coherence of healthy control participants. The third specific aim includes identifying the number of muscle networks necessary to explain isometric force generation in stroke patients and healthy controls as well numerically quantifying these networks with graph theory measures to further explain the implications of these emergent muscle networks.

CHAPTER 2 – MATERIALS AND METHODS

2.1 Participants and Demographics

Eight mild post-stroke survivors, eight moderate post-stroke survivors, ten severe post-stroke survivors, with either single hemorrhagic stroke or ischemic stroke, and six age-matched healthy participants were recruited. Healthy participants were neurologically healthy and possessed neither muscular nor orthopedic impairments of upper limbs. Stroke survivor demographics and clinical scores are noted in Table 1. Surface electromyography of the affected limb was assessed in the stroke survivors (eight/eight/ten datasets) whereas both limbs of healthy participants were assessed (twelve datasets). Stroke survivor demographics and Fugyl-Meyer Assessment (FMA) clinical scores are adapted from *Roh et al.*. The FMA score is an index used to quantify the extent of sensory-motor capacity following a stroke. FMA is also a good indicator of post-stroke recovery with motor rehabilitation. The FMA scale is subdivided into the following categories: motor function (upper and lower limb), sensory function, balance, range of motion of joints, and joint pain. In Table 1 the score for the entire assessment (/66) as well as the sub-scores for individual tests related to elbow and shoulder functionality (/22) are implemented. The study was performed in accordance with the Declaration of Helsinki, with the approval of the Northwestern University Institutional Review Board. Each participant gave informed consent before testing.

Table 1. Participant Demographics and Clinical Scores.

		Mean	SD	Range
Hemiparetic group (n = 24)				
Mildly impaired (n = 8)				
Age (yrs)		55.6	9.5	46-70
Months post-stroke		51.0	24.6	23-89
FMA score (/66)		55.3	5.3	50-66
FMA score (/22)		19.6	2.3	16-22
Sex (M/F)	5/3			
Affected side (L/R)	2/6			
Moderately impaired (n = 8)				
Age (yrs)		56.0	8.7	44-68
Months post-stroke		82.1	60.0	21-179
FMA score (/66)		36.1	7.0	29-45
FMA score (/22)		16.1	22	13-19
Sex (M/F)	6/2			
Affected side (L/R)	4/4			
Severely impaired (n = 8)				
Age (yrs)		61.8	10.0	53-81
Months post-stroke		174.8	94.7	68-302
FMA score (/66)		17.5	3.8	12-23
FMA score (/22)		10.3	1.6	8-12

Table 1 continued.					
Sex (M/F)	3/5				
Affected side (L/R)	3/5				
Control group (n = 6)					
Age			63.2	7.6	52-73
Sex (M/F)	4/2				

2.2 Data Acquisition

Hand position and 3D forces generated at the hand were recorded using the Multi-Axis Cartesian-based Arm Rehabilitation Machine (MACARM). The MACARM is a cable-robot designed for upper limb motor rehabilitation (Mayhew et al., 2005; Beer et al., 2008). Forces, arm orientation, and handle position were sampled at 64 Hz. sEMG were recorded (Bagnoli 8; Delsys, Boston, MA) from eight elbow and shoulder muscles: brachioradialis (BRD), biceps brachii (BIm), triceps brachii, long and lateral heads (TRIlong & TRIlat, respectively), anterior, middle, and posterior deltoid fibers (AD, MD, PD, respectively), and the pectoralis major (PECTclav). sEMG signals were amplified (x1000), online band-pass filtered (20-450 Hz), and sampled at 1920 Hz. Data acquisition between the MACARM and sEMG amplifier were synchronized with a common clock and trigger.

2.3 Experimental Design

Participants voluntarily generated forces in a self-paced manner in 54 different directions approximately distributed uniformly in 3D force space while grasping the gimbaled handle of the MACARM with their hand in front of the ipsilateral shoulder.

8

The high number of targets in multiple directions ensures robustness of muscle synergy analysis by observing co-activation of muscles in a wider range of motion such that the results are not biased towards a specific direction. Force magnitude was set at 40% maximum lateral force for all subjects. A successful trial required for the participant to match a cursor to a target sphere for at least 800 milliseconds. Stroke patients performed the task with their affected limb while healthy controls performed the task with both arms. An intertrial interval of 10 seconds and a 1-minute resting period were introduced to avoid muscle fatigue. All participants were right-hand dominant. An illustration of the target reaching protocol is presented below in Figure 1. The red sphere indicates the starting position for the hand in force generation. The blue spheres are the different targets which must be reached by the subjects.
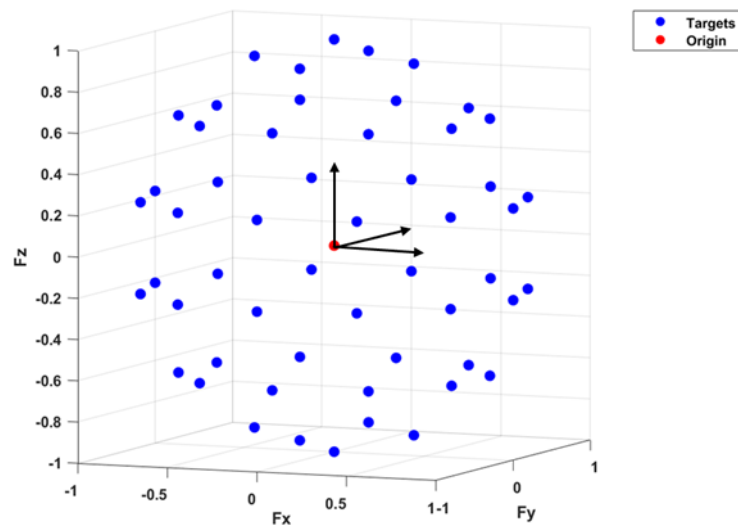
Figure 1. Experimental Setup. 54 targets in 3D Cartesian space approximately normally distributed.

2.4 Data Analysis

First, the isometric contraction phase of each trial was extracted. The data was then further demeaned, rectified via the Hilbert transform, and normalized to unit variance to prevent subsequent analyses to be biased by high-variance muscles. Signals from all trials were then concatenated in order to provide more samples for time-frequency analysis. The Hilbert transform yields the complex-valued analytic signal,

$$A_H = \sqrt{x^2 + \tilde{x}^2} \qquad (1)$$

composed of the original signal, x, and a 90° phase shifted version of the original signal, $\tilde{x}$. Rectification via the Hilbert transform produces similar results to full-wave rectification (Myers et al., 2003; Boonstra et al., 2012). The instantaneous amplitude of the sEMG was recovered from the Hilbert amplitude. Power spectral density (PSD) of the normalized sEMG envelopes was determined using the modified Welch periodogram. PSD is the measure of a signal's power content observed at discrete frequencies. A Hanning window with a length of 500 milliseconds and 50% overlap was applied in the frequency range of 0 – 50 Hz with a spectral resolution of 2 Hz. Intermuscular coherence of the eight upper-arm muscles was calculated via the magnitude-squared coherence. The formula for magnitude-squared coherence is

$$C(f)^2_{xy} = \frac{|P_{xy}|^2}{P_{xx} x P_{yy}}, \qquad (2)$$

where it is derived by calculating the cross-spectrum between two signals, P_{xy}, and normalizing it to the signals' auto-spectra, P_{xx} and P_{yy}. Coherence was calculated from

0 – 50 Hz with a window size of 500 milliseconds and 50% overlap resulting in a frequency resolution of 2 Hz.

After calculating intermuscular coherence for every muscle combination (28 pairs), coherence matrices were subjected to non-negative matrix factorization (NNMF). NNMF returns a lower-rank approximation of input data and is akin to principal component analysis except with the added non-negative constraints. NNMF was implemented to identify unique spectral patterns shared by muscles in the coherence matrices. NNMF returns weight coefficients (strength of muscle contribution) and activation patterns (identified patterns in coherence). Coherence was modeled as a k-ranked reconstruction matrix, M, with residual reconstruction error matrix E

$$M_{f \, x \, m} = W_{f \, x \, k} \, x \, H_{k \, x \, m} + E_{f \, x \, m}. \tag{3}$$

M has dimensions: f the number of frequencies where coherence is evaluated, m the total number of muscle pairs, and k being the requested matrix rank. This resulted in two matrices, W and H.

Since the number of unique muscle networks needed to explain the force generation is unknown prior to analysis, variance accounted for (VAF) was used to determine the minimum number of muscle networks necessary to explain intermuscular coherence with a threshold of 90% of VAF (Wojtara et al., 2014). VAF describes how well the results from NNMF can describe the variance of the input data. VAF was calculated using the Frobenius norms of the error matrix E and reconstruction matrix M

11

$$VAF = 1 - \frac{|E|^2_{fro}}{|M|^2_{fro}}, \qquad (4)$$

where the error matrix E is equal to the reconstruction matrix M subtracted from the original coherence matrix. These activation patterns parsed from the coherence matrix are the unique frequency patterns shared by sets of muscles during the force generation period. The weight coefficients are taken to be the undirected weighted functional connectivity matrices. Functional connectivity matrices where thresholded only for visual inspection using the minimum-spanning tree algorithm.

Graph theory measures were calculated from normalized functional connectivity matrices. The betweenness centrality (BC), clustering coefficient (CC), global efficiency (GE), and node strength (NS) were compared between healthy participants and stroke survivors. BC is a measure of the degree of a node being in-between other nodes and is calculated using the number of shortest path lengths passing through the node of interest. The CC is a network measure of how likely it is for nodes of interest to cluster together. GE is the average inverse shortest path length in the network. NS is a measure of the participation of a node and is calculated by summing the edge weights connected to the node of interest.

Additionally, the means of power spectral density and intermuscular coherence in the δ (0-4 Hz), θ (4-8 Hz), α (8-13 Hz), β (13-30 Hz), and γ (30-50 Hz) bands were statistically compared via a One-Way Analysis of Variance (ANOVA) with a pre-set alpha level of 0.05. Prior to statistical testing, coherence values were further normalized via the hyperbolic tangent transformation to facilitate statistical comparison across participants and groups

$$Z = tan^{-1}\left(\sqrt{C_{xy}}\right) \times \sqrt{L}, \tag{5}$$

where L is the number of disjoint sections used in the calculation of intermuscular coherence. ANOVA tests resulting in significant differences of the mean were followed up with a multiple comparison test using Tukey's Honestly Significant Difference Procedure. All ANOVA tests were balanced studies, such that an equal number of subjects were used (eight datasets per group). All offline data processing was conducted within the MATLAB environment. All network visualization and graph theory analysis were performed using the Brain Connectivity Toolbox (Rubinov and Sporns, 2010). A general overview of the entire data processing can be found in Figure 2 below.
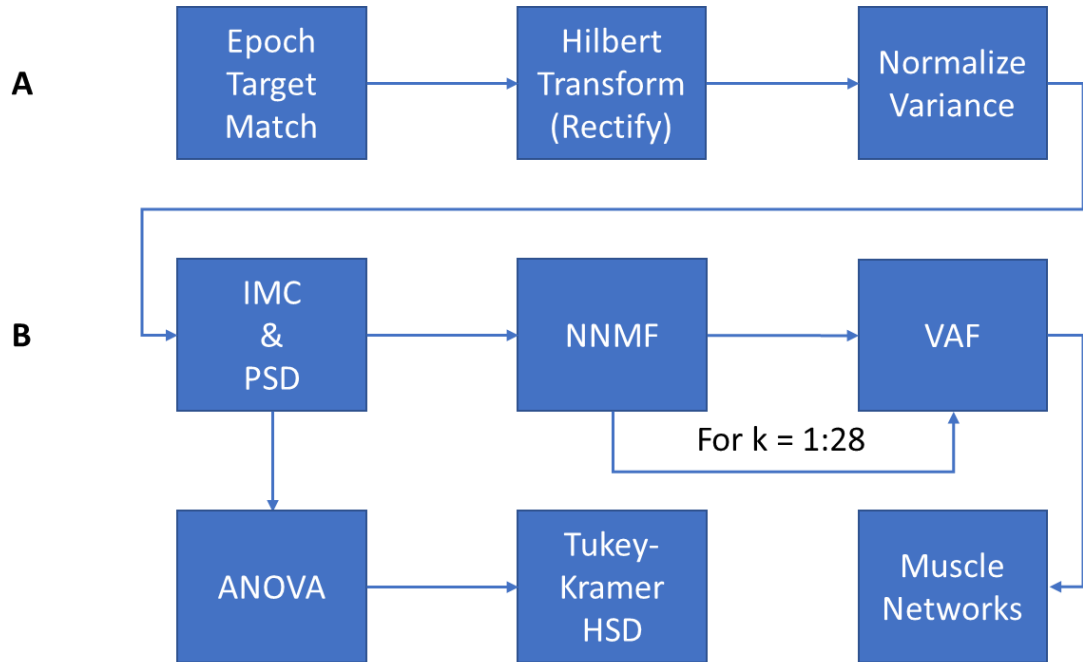

Figure 2. EMG Processing Pipeline. (A) EMG pre-processing steps. (B) EMG post-processing, including statistical tests and coherence muscle network analysis.

CHAPTER 3 – RESULTS

3.1 Power Spectral Density

The normalized power spectral density of EMG collected during the isometric force generation period reveals some significant differences in frequency content between the healthy controls and chronic stroke survivors. As seen in Figure 3, healthy controls exhibit a higher magnitude of PSD at most frequencies in normalized EMG envelopes in the range of $0 - 50$ Hz. Overall, there are four distinct spectral peaks visible, namely, δ, α, β, and γ. Healthy controls exhibited greater magnitude PSD in the α band in BIm, TRIlong, TRIlat, PD, and PECTclav. Healthy controls also showed greater magnitude PSD versus mild and moderate impairment stroke in the β and γ bands overall in TRIlong, TRIlat, AD, MD, PD, and PECTclav. Surprisingly, severe impairment stroke patients displayed similar or higher magnitude of PSD in β and γ bands for TRIlong, AD, PD, and PECTclav. These underlying differences in the frequency domain serve as the foundation for future multi-group differences in coherence and functional connectivity analysis.
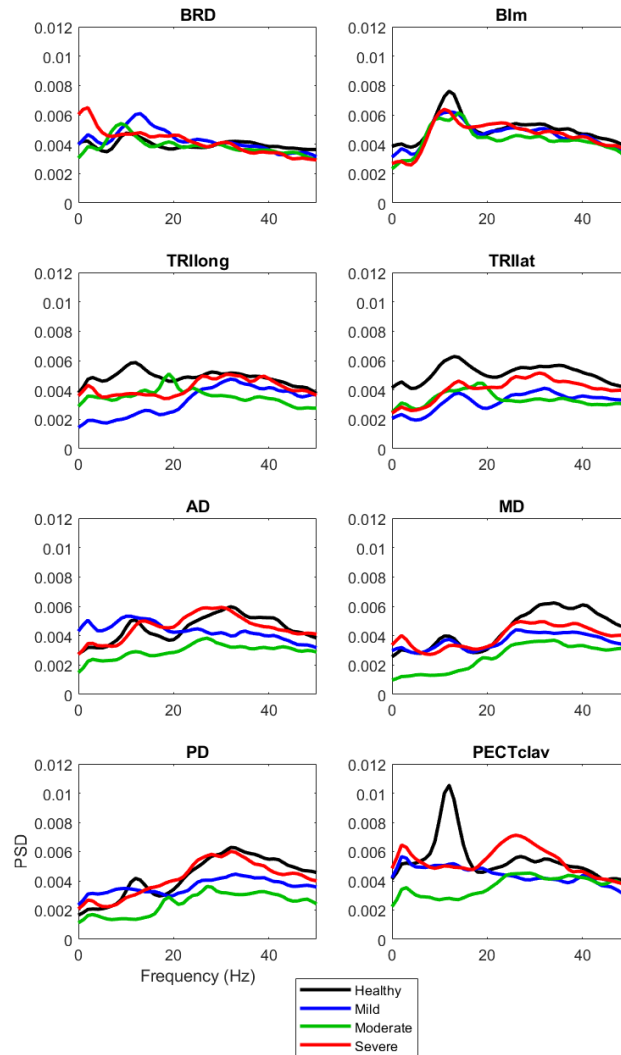
Figure 3. Normalized Welch PSD for Healthy Controls & Multi-Severity Stroke Groups.

Since some clear spectral differences in the PSD are observed visually, the mean value of PSD in the δ, θ, α, β, and γ frequency bands were extracted in order to make a multi-group statistical comparison. One-way ANOVA p-values are reported in Table 2. Table 2 shows significant differences were revealed primarily in the higher frequency bands including α, β, and γ. Most of the significant differences manifested in the triceps, deltoids, and pectoralis muscles. Very few statistical differences were

15

observed in the lower δ and θ frequency bands and were only found in the triceps muscles. ANOVA tests resulting in significant differences were followed up with multiple-comparisons tests to verify which groups were statistically different from each other. Tables of multiple-comparison test results include the frequency bands of interest, p-values, and mean group differences to identify which group has higher or lower PSD values compared to the other group.

Table 2. ANOVA p-values for Normalized Welch PSD. Alpha level set at 0.05. Significant p-values are marked with asterisks.

	BRD	BIm	TRIlong	TRIlat	AD	MD	PD	PECTclav
δ	0.1206	0.3051	0.0147*	0.0590	0.1438	0.2361	0.2002	0.2041
θ	0.5619	0.8303	0.0060*	0.0224*	0.2496	0.2178	0.1314	0.3628
α	0.9672	0.8680	0.0015*	0.0383*	0.2196	0.1690	0.0495*	0.0176*
β	0.7134	0.6705	0.0288*	0.0299*	0.0283*	0.0352*	0.0062*	0.0127*
γ	0.5298	0.7181	0.0069*	0.0035*	0.0035*	0.0007*	0.0017*	0.3236

Table 3 displays the muscles indicating significant differences in the mean PSD in specific frequency bands for healthy controls versus the mild, moderate, and severe impairment stroke groups. Healthy controls had significantly higher mean PSD in all frequency bands compared to both the mild and moderate impairment stroke severity groups. However, no statistically significant differences in mean PSD were observed for healthy control group versus the chronic severe impairment stroke group. The long and lateral triceps heads held consistent differences in healthy versus mild impairment stroke patients. Healthy controls exhibited significantly higher mean PSD values in

higher frequency bands compared to moderate impairment stroke patients in the long

and lateral triceps heads along with the anterior, middle, and posterior deltoid fibers.

Table 3. Multiple Comparisons Test for Normalized Welch PSD in Healthy vs Multi-Severity Stroke Groups.

Group 1 vs. Group 2	Frequency Band	Muscle	p-value	Group 1 M +/- SD	Group 2 M +/- SD
Healthy vs. Mild					
	δ	TRIlong	0.0114	0.0055 +/- 0.0022	0.0018 +/- 0.0013
	θ	TRIlong	0.0032	0.0059 +/- 0.0021	0.0018 +/- 0.0013
		TRIlat	0.0164	0.0051 +/- 0.0024	0.0021 +/- 0.0007
	α	TRIlong	0.0008	0.0069 +/- 0.0023	0.0022 +/- 0.0014
		TRIlat	0.0352	0.0067 +/- 0.0033	0.0031 +/- 0.0012
	β	TRIlong	0.0178	0.0056 +/- 0.0014	0.0032 +/- 0.0010
		TRIlat	0.0317	0.0060 +/- 0.0018	0.0034 +/- 0.0010
	γ	TRIlat	0.0359	0.0050 +/- 0.0011	0.0036 +/- 0.0008
		MD	0.0105	0.0058 +/- 0.0014	0.0039 +/- 0.0009
Healthy vs. Moderate					
	α	TRIlong	0.0244	0.0069 +/- 0.0023	0.0036 +/- 0.0025

Table 3 continued.

	PD	0.0369	0.0042 +/- 0.0027	0.0014 +/- 0.0009
	PECTclav	0.0101	0.0092 +/- 0.0062	0.0028 +/- 0.0022
β	**PD**	0.0346	0.0045 +/- 0.0012	0.0026 +/- 0.0013
γ	**TRIlong**	0.0206	0.0045 +/- 0.0009	0.0032 +/- 0.0009
	TRIlat	0.0042	0.0050 +/- 0.0011	0.0032 +/- 0.0011
	AD	0.0039	0.0049 +/- 0.0013	0.0031 +/- 0.0007
	MD	0.0005	0.0058 +/- 0.0014	0.0033 +/- 0.0011
	PD	0.0017	0.0056 +/- 0.0011	0.0030 +/- 0.0016

Table 4 below holds the multiple-comparisons test results for stroke group comparisons of mean PSD values in different spectral ranges. Significant group differences were only observed in moderate versus chronic severe impairment stroke patients. The long and lateral triceps heads repeatedly showed significant statistical differences in the β and γ bands. Severe impairment stroke patients maintained higher average PSD values compared to the moderate impairment stroke patients.

18

Table 4.Multiple Comparisons Test for Normalized Welch PSD in Multi-Severity Stroke Comparison.

Group 1 vs. Group 2	Frequency Band	Muscle	p-value	Group 1 M +/- SD	Group 2 M +/- SD
Moderate vs. Severe					
	β	TRIlong	0.0114	0.0031 +/- 0.0012	0.0054 +/- 0.0013
		TRIlong	0.0032	0.0026 +/- 0.0013	0.0049 +/- 0.0015
		TRIlat	0.0164	0.0037 +/- 0.0012	0.0064 +/- 0.0023
	γ	TRIlong	0.0008	0.0032 +/- 0.0009	0.0047 +/- 0.0008
		TRIlat	0.0352	0.0031 +/- 0.0007	0.0046 +/- 0.0009
		TRIlong	0.0178	0.0030 +/- 0.0016	0.0051 +/- 0.0007

3.2 Intermuscular Coherence

Observing intermuscular coherence during the isometric force generation period in Figure 4 it is apparent that the magnitude of coherence tends to be reduced in post-stroke survivors compared to healthy individuals in most of the muscle pairs. There are, however, few muscle pairs where coherence of stroke survivor muscles are similar magnitude to the coherence of healthy controls, and few muscle pairs where stroke survivors exhibit slightly greater coherence versus healthy controls.
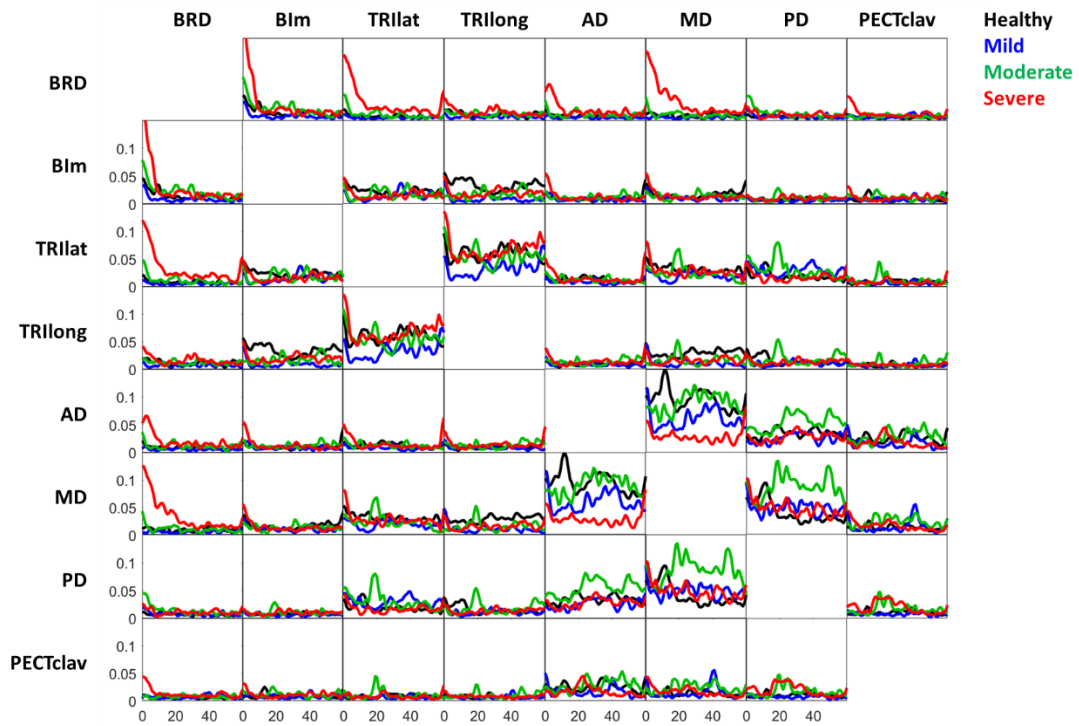
Figure 4. Average Intermuscular Coherence for Healthy Controls & Multi-Severity Stroke Groups.

Visually, the most different aspect of coherence between healthy controls and stroke survivors is within the AD-MD, MD-PD, and TRIlong-TRIlat muscle-pairs. As the severity of stroke impairment increases, the magnitude of coherence in the AD-MD connection decreases. Healthy controls and mild impairment stroke patients hold similar values in the β and γ bands. Healthy controls also maintain higher coherence in the α band versus all levels of stroke impairment. Moderate impairment stroke displayed greater broadband coherence from α to γ bands versus all other groups in the MD-PD connection. Severe impairment stroke patients displayed greater coherence in the δ band for the following muscle pairs: BRD-BIm, BRD-TRIlat, BRD-AD, BRD-MD, and BRD-PECTclav.

Average coherence values in the δ, θ, α, β, and γ bands were extracted and compared with One-Way ANOVA statistical tests for quantitative analysis following normalization via the hyperbolic tangent transformation. Table 5 below holds the p-values from ANOVA testing. Muscle-pairs with significant differences in the mean normalized coherence are indicated with asterisks.

Table 5. ANOVA p-values for Normalized Coherence. Alpha level set at 0.05. Significant p-values are marked with asterisks.

	δ	θ	α	β	γ
BRD-BIm	0.7589	0.8154	0.7279	0.6119	0.6329
BRD-TRIlong	0.0410*	0.0630	0.1180	0.1758	0.1075
BRD-TRIlat	0.2379	0.3117	0.1335	0.2414	0.5728
BRD-AD	0.2292	0.2985	0.2183	0.4656	0.3730
BRD-MD	0.0312*	0.0223*	0.0521	0.0391*	0.2859
BRD-PD	0.6233	0.2967	0.5088	0.5898	0.3559
BRD-PECTclav	0.3521	0.1650	0.7811	0.6732	0.6357
BIm-TRIlong	0.1268	0.0755	0.0432*	0.2992	0.7231
BIm-TRIlat	0.1386	0.0124*	0.0555	0.1021	0.3298
BIm-AD	0.5049	0.9086	0.9258	0.9988	0.2646
BIm-MD	0.6471	0.9461	0.4979	0.9660	0.6106
BIm-PD	0.5464	0.3118	0.8111	0.2576	0.5408
BIm-PECTclav	0.7265	0.5158	0.0723	0.3560	0.7462
TRIlong-TRIlat	0.1104	0.1508	0.1556	0.6552	0.8910
TRIlong-AD	0.3579	0.6533	0.4472	0.2924	0.6598

Table 5 continued.

TRIlong-MD	0.4929	0.4426	0.4091	0.3906	0.7224
TRIlong-PD	0.6609	0.6945	0.0035*	0.3137	0.3906
TRIlong-PECTclav	0.2848	0.8471	0.0691	0.4401	0.3453
TRIlat-AD	0.5596	0.8362	0.3420	0.8932	0.6596
TRIlat-MD	0.1286	0.0406*	0.4338	0.4477	0.4323
TRIlat-PD	0.2506	0.4753	0.2845	0.3329	0.4608
TRIlat-PECTclav	0.4385	0.6395	0.3955	0.2367	0.9523
AD-MD	0.0697	0.0022*	0.0004*	0.0005*	0.0186*
AD-PD	0.8356	0.7416	0.6984	0.1765	0.0570
AD-PECTclav	0.2340	0.2229	0.2356	0.7751	0.2733
MD-PD	0.9629	0.6531	0.3382	0.4589	0.0920
MD-PECTclav	0.5103	0.8717	0.8468	0.7661	0.4195
PD-PECTclav	0.3927	0.8549	0.0440*	0.2306	0.0315*

Only two muscle-pairs held significant differences in δ band coherence, namely BRD-TRIlong and BRD-MD. BRD-MD, BIm-TRIlat, TRIlat-MD, and AD-MD muscle pairs suggested significant difference in coherence in the θ band. The α band presented significant difference in mean normalized coherence for BIm-TRIlong, TRIlong-PD, AD-MD, and PD-PECTclav. Only two muscle pairs were found to have significant differences in the β band, including BRD-MD and AD-MD. Lastly, AD-MD and PD-PECTclav showed significant differences in the γ band. All of the previously mentioned combinations of muscle-pairs and frequency bands were

submitted to multiple-comparisons tests to identify which groups were significantly different from others.

Table 6 displays the results from multiple-comparisons test for healthy controls versus mild, moderate, and severe impairment stroke patients. Healthy controls were found to have significantly greater coherence in the θ and α bands for the AD-MD connection versus mild impairment stroke patients. Healthy controls also displayed greater θ band coherence in the BIm-TRIlat connection compared to mild and moderate impairment stroke patients. Most of the significant differences in mean normalized coherence were identified when comparing healthy controls to severe impairment stroke patients. AD-MD was consistently different for θ, α, β, and γ bands when comparing healthy controls to chronic severe stroke patients.

Table 6. Multiple Comparisons Tests for Normalized Coherence in Healthy vs. Multi-Severity Stroke Groups.

Group 1 vs. Group 2	Frequency Band	Muscle-Pair	p-value	Group 1 M +/- SD	Group 2 M +/- SD
Healthy vs. Mild					
	θ	BIm - TRIlat	0.0169	3.8130 +/- 2.8788	1.3759 +/- 0.5061
		AD-MD	0.0261	6.7441 +/- 2.6637	3.5110 +/- 2.1293
	α	AD-MD	0.0056	7.7766 +/- 3.0605	3.7034 +/- 2.1698
Healthy vs. Moderate					
	θ	BIm - TRIlat	0.0272	3.8130 +/- 2.8788	1.5284 +/- 0.6039

Table 6 continued.					
	α	**AD-MD**	0.0397	7.7766 +/- 3.0605	4.6128 +/- 2.0332
Healthy vs. Severe					
	θ	**TRIlat - MD**	0.0315	3.1600 +/- 2.0508	1.5369 +/- 0.4842
		AD-MD	0.0014	3.8130 +/- 2.8788	2.2540 +/- 1.2560
	α	**TRIlong - PD**	0.0018	4.0125 +/- 1.3005	1.6851 +/- 0.7674
		AD-MD	0.0002	7.7766 +/- 3.0605	2.3820 +/- 1.3149
	β	**AD-MD**	0.0008	5.7433 +/- 1.9836	2.1003 +/- 0.4424
	γ	**AD-MD**	0.0489	5.3501 +/- 2.3159	1.8488 +/- 0.6250

Stroke groups were also compared to each other with multiple-comparisons tests and the results are displayed in Table 7. Moderate impairment stroke patients showed increased γ band coherence versus mild impairment stroke patients in the PD-PECTclav connection. Chronic severe impairment stroke patients displayed greater magnitude coherence in the δ, θ, and β bands for BRD-MD compared to mild impairment stroke patients. Lastly, Severe impairment stroke patients had higher θ band coherence versus moderate impairment stroke patients for BRD-MD muscle pair however moderate impairment stroke patients showed greater β and γ band coherence versus severe impairment stroke patients in the AD-MD connection.

Table 7. Multiple Comparisons Test for Normalized Coherence in Multi-Severity Stroke Groups.

Group 1 vs. Group 2	Frequency Band	Muscle-Pair	p-value	Group 1 M +/- SD	Group 2 M +/- SD
Mild vs. Moderate					
	γ	**PD - PECTclav**	0.0314	1.4698 +/- 0.2009	2.107 +/- 0.6504
Mild vs. Severe					
	δ	**BRD-MD**	0.0346	1.2047 +/- 0.3090	5.8007 +/- 5.9314
	θ	**BRD-MD**	0.0449	1.4256 +/- 0.5555	4.4633 +/- 4.1800
	β	**BRD-MD**	0.0350	1.2332 +/- 0.1645	2.7546 +/- 1.9885
Moderate vs. Severe					
	θ	**BRD-MD**	0.0301	1.2322 +/- 0.7365	4.4633 +/- 4.1800
	β	**AD-MD**	0.0021	5.4413 +/- 1.5300	2.1003 +/- 0.4424
	γ	**AD-MD**	0.0191	5.6350 +/- 2.6414	1.8488 +/- 0.6250

3.3 Number of Networks Needed

Variance explained from spectral coherence patterns extracted by NNMF indicated different minimum number of muscle networks necessary to explain coherence patterns across groups. Healthy controls exhibited distinct functional muscle association in four distinct spectral ranges (H1-H4) whereas post-stroke

survivors showed less functional connectivity. Mild stroke patients exhibited functional connectivity in three spectral ranges (I1-I3). Moderate and chronic severe stroke patients were observed to possess coherence in only two spectral ranges (O1-O2 and S1-S2, respectively). Figure 5 demonstrates the change in magnitude of variance explained in coherence with increasing number of spectral patterns identified from coherence.
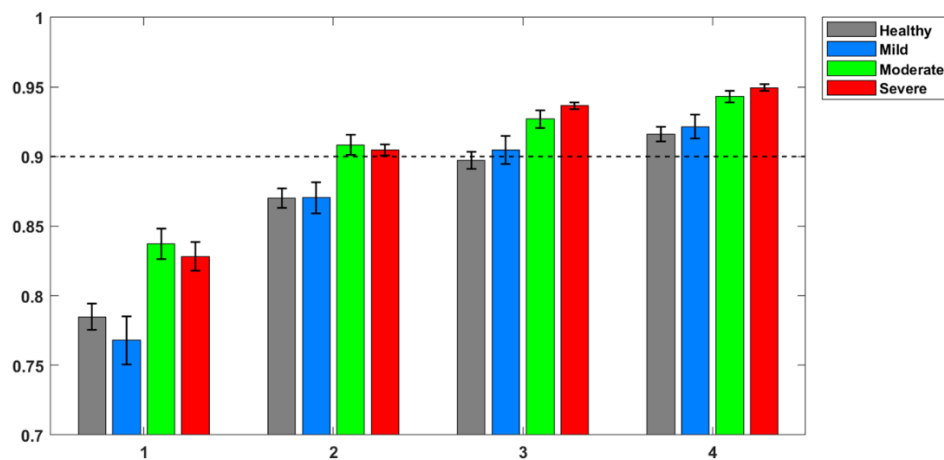

Figure 5. Variance Accounted For (VAF). Error bars indicate standard error of the mean. Threshold set at 0.9.

3.4 Muscle Network Topology

Visualizing the network backbones for isometric force generation shows the dominant network edges and gives a basic indication as to which muscles are more important to the network. For all figures displaying functional muscle networks the left-hand column contains the coherence patterns identified from NNMF in increasing order of spectral content, the middle column holds thresholded connectivity matrices and the right-most column shows the network topology corresponding to a specific coherence pattern and functional connectivity matrix. Edge weights are plotted as "low" (dashed), "medium" (thin), and "high" (thick) strengths proportional to the

maximum edge weight per network per group. Network labels are also provided toward the left-hand side of the coherence patterns. Figure 6 highlights the network backbones of healthy muscle networks. The healthy muscle networks' peak spectral patterns lie in the δ and θ bands, α band, β band, and γ bands. The H1 network includes BRD-BIm, TRIlat-TRIlong, BIm-TRIlat, AD-MD, and MD-PD as high strength edges. AD-MD and MD-PD appear as high strength edges once again in the H2 network. The only high strength edges within the H3 and H4 networks is AD-MD.
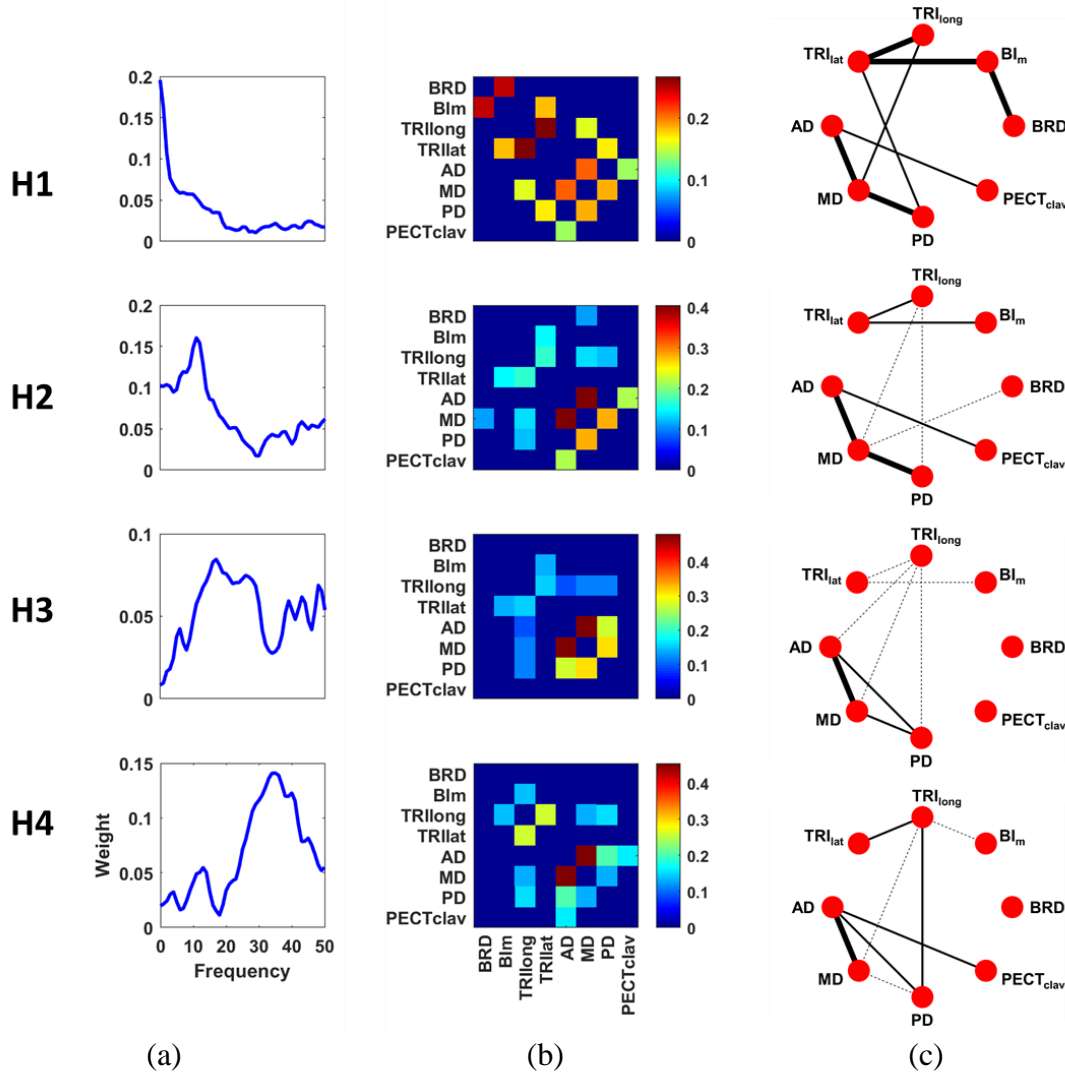

Figure 6. Healthy Muscle Networks. (a) Coherence Patterns. (b) Connectivity Matrices. (c) Network Topology.

27

Figure 7 depicts the mild stroke muscle networks network backbones. The mild stroke muscle networks seem to focus on combined δ and θ bands, combined α and β bands, and the γ band. AD-MD and MD-PD reappear as high strength edges in the I1 and I2 functional muscle networks. BIm-TRIlong, TRIlat-TRIlong, TRIlong-PD, AD-MD, and MD-PECTclav are the dominant edges in the I3 network.
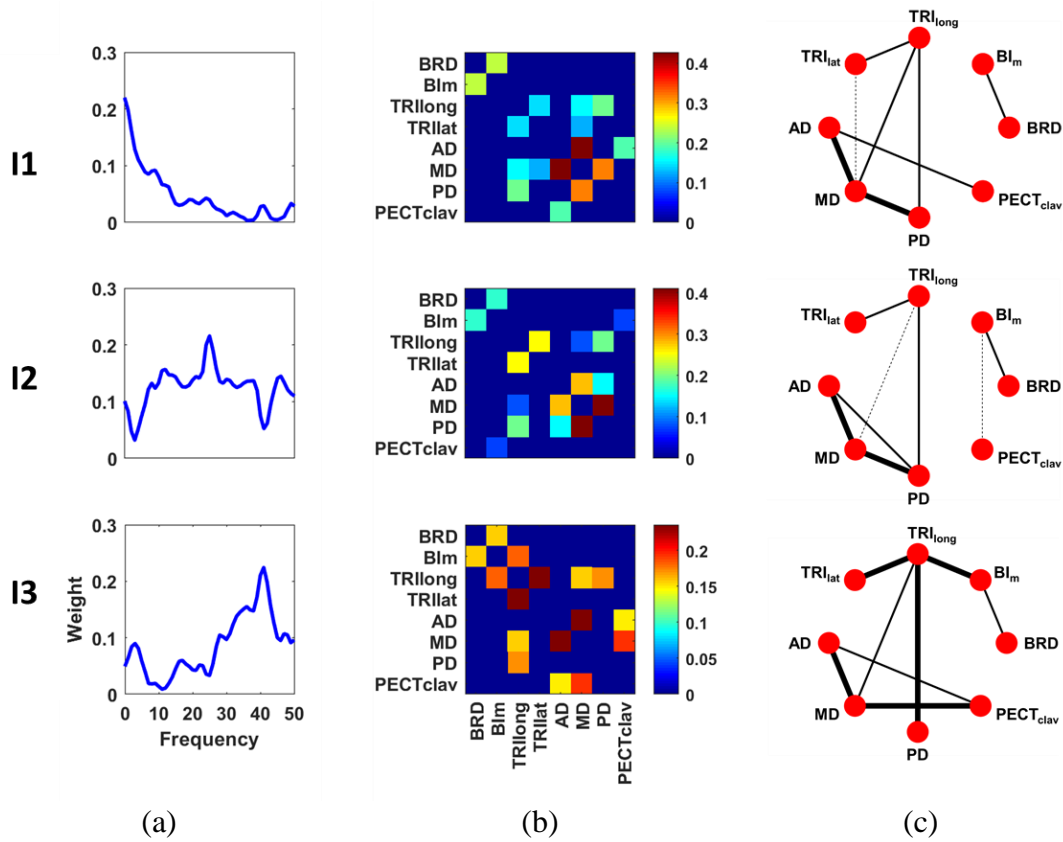

(a)　　　　　　　　　　(b)　　　　　　　　　　(c)

Figure 7. Mild Stroke Muscle Networks. (a) Coherence Patterns. (b) Connectivity Matrices. (c) Network Topology.

Figure 8 depicts the moderate stroke muscle networks network backbones. The coherence patterns extracted from moderate impairment stroke survivors are much simpler in comparison to that of the healthy controls. The frequency content of the stroke muscle networks peaks in the combined δ, θ, and α bands for network O1 and the combined β and γ bands for network O2. BIm-BRD, TRIlat-TRIlong, and AD-MD

28

appear as the dominant edges in the O1 network whereas AD-MD, AD-PD, and MD-PD are the high strength edges in the O2 network.

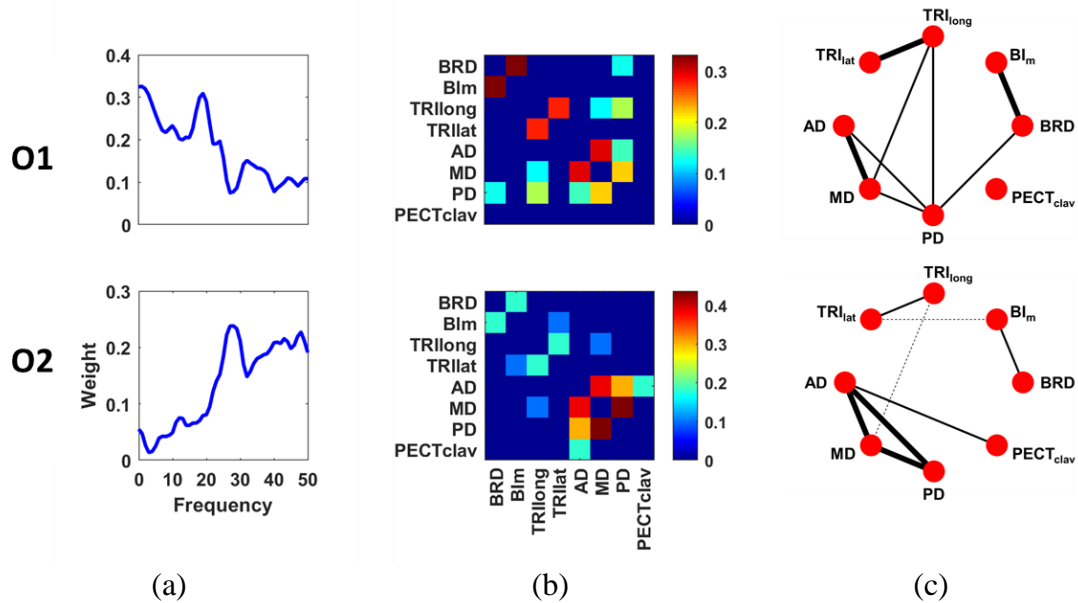(a)   (b)   (c)

Figure 8. Moderate Stroke Muscle Networks. (a) Coherence Patterns. (b) Connectivity Matrices. (c) Network Topology.

Figure 9 depicts the severe stroke muscle networks network backbones. The coherence pattern associated with the S1 network peaks in the combined δ and θ bands. The S2 network is concentrated mostly in the β bands with some small spillover into low γ spectral range. High strength edges in the S1 network include BRD-BIm and TRIlat-TRIlong. High strength edges in the S2 network include TRIlat-TRIlong and MD-PD.
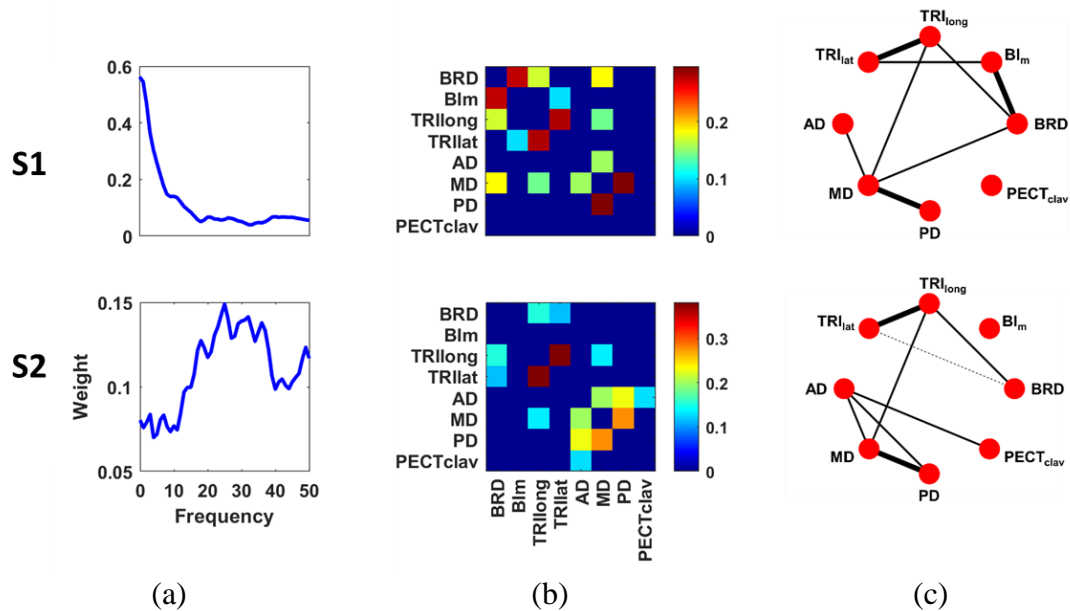
Figure 9. Severe Stroke Muscle Networks. (a) Coherence Patterns. (b) Connectivity Matrices. (c) Network Topology.

3.5 Network Metrics
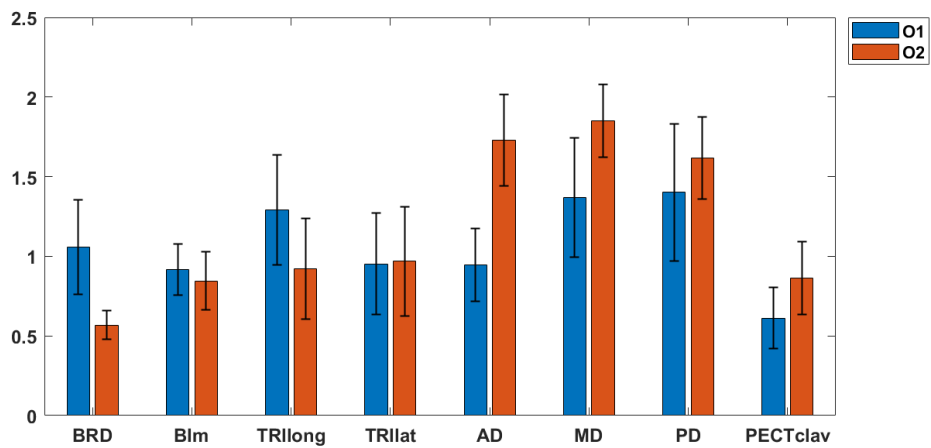
The functional muscle networks were quantified via graph theory analysis to better explain the contribution of each individual muscle to the entire network. Error bars in Figure 10 reflect the standard error of the means (SEM) of the network metrics.
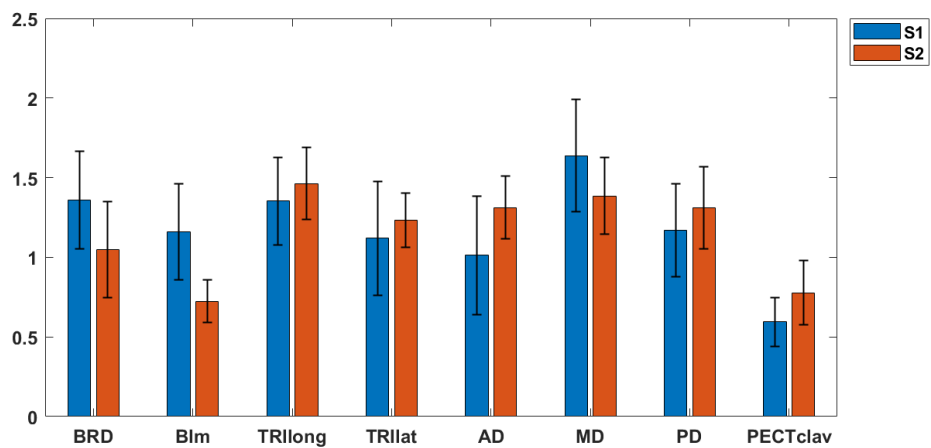

(a)
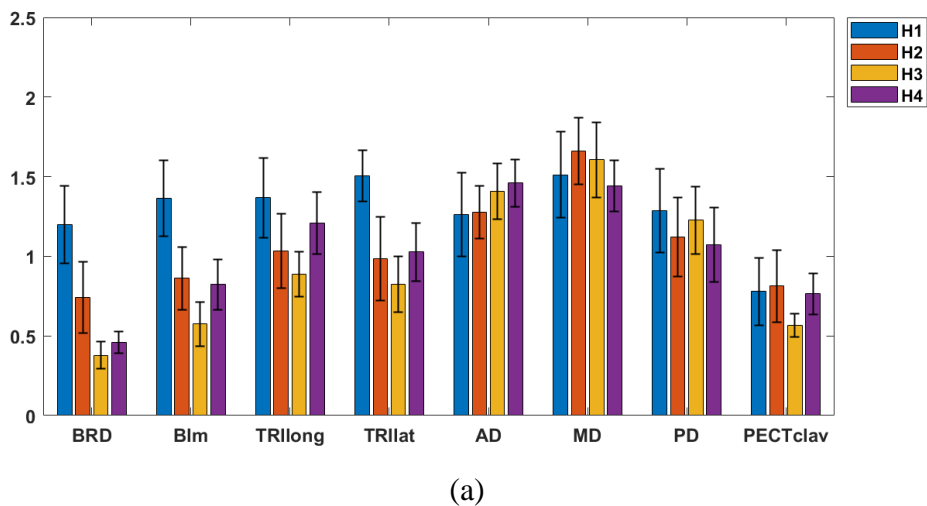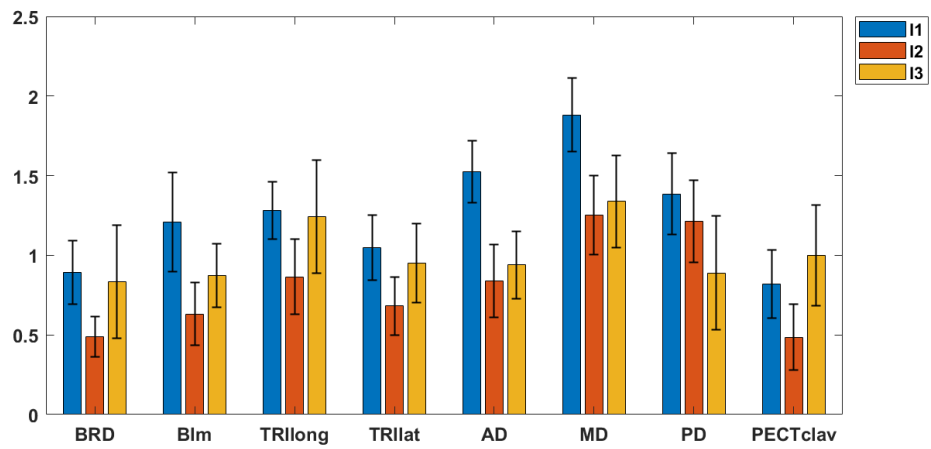
(b)

(c)

(d)

Figure 10. Node Strength Network Metric. (a) Healthy. (b) Mild Stroke. (c) Moderate Stroke. (d) Severe Stroke.

The node strength network metric derived from isometric force generation give an insight into which muscles participate the most as nodes in the network. For the healthy controls, the H1 network showed the BRD, BIm, TRIlong, TRIlat, AD, MD, and PD nodes to have the highest node strength on average. The H2 network included the AD, MD, and PD nodes with higher node strength. In the H3 network the AD, MD, and PD nodes all have the higher magnitude node strength. The H4 network node strength is dominated once again with AD and MD nodes. Overall, the AD, MD, and PD muscles seem to be the dominant nodes with the most node strength, especially as the frequency content of coherence patterns increases.

In mild stroke muscle networks, nodes AD and MD seem to have the most node strength in the I1 networks. MD and PD nodes hold the higher node strength in the I2 network. Nodes TRIlong and MD have the most node strength in the I3 network. In moderate stroke muscle networks, TRIlong, MD, and PD seem to dominate the node strength of the O1 network whereas AD, MD, and PD contribute the most towards the O2 network node strength. For severe stroke muscle networks BRD, TRIlong, and MD are the nodes with more node strength in the S1 network. TRIlong, AD, MD, and PD nodes have the most node strength in the S2 network.

CHAPTER 4 – DISCUSSION

4.1 Reduced Power Spectral Density Post-Stroke

The power spectral density observed from chronic stroke survivors as compared to healthy controls reveals the initial differences in the frequency domain that prelude the differences in functional muscle connectivity revealed by intermuscular coherence. As evidenced in the results, the magnitude of power spectral density was reduced overall post-stroke. This change in power spectral density was most evident in the higher frequency bands, namely: α, β, and γ. The reduction in power spectral density was noticeable in the TRIlat, TRIlong, AD, MD, and PD muscles with ANOVA. PSD in healthy controls were found to be statistically significantly higher versus mild and moderate impairment stroke patients but no statistically significant difference was found between the healthy controls and chronic severe stroke patients. However, severe stroke patients were found to have significantly higher β and γ band PSD versus moderate stroke patients primarily in the AD and PD muscles.

Overall, the results of statistical comparison of normalized power spectral density indicates that the triceps heads and deltoid fibers tend to show the most difference in the frequency domain when comparing healthy controls and stroke patients of multiple impairment levels. This reduction in power spectral density post-stroke is consistent with other findings in literature with the interosseous muscle of stroke patients (Li et al., 2014).

4.2 Reduced Intermuscular Coherence Post-Stroke

Simplified functional muscle connectivity was observed in the chronic stroke survivors during isometric force generation as compared to the healthy controls.

33

Healthy controls exhibited functional connectivity at four distinct spectral bands: combined δ and θ, α, β, and γ. Stroke survivors presented with reduced functional connectivity in the β and γ bands primarily. Several synergistic muscle-pairs previously identified by *Roh et al.* appear to be highly coherent, such as TRIlat-TRIlong, AD-MD, AD-PD, and MD-PD. The BRD-BIm muscle-pair is one common synergy for both healthy controls and stroke patients of any severity that do not appear to have much coherence at any frequency except for the lower frequencies of the δ band. The synergistic AD-MD muscle pair proved to have the most statistically significant differences in the mean of normalized coherence from the θ band all the way to the γ band. However, there were a few non-synergistic muscle-pairs that also indicated some statistically significant differences in mean normalized coherence.

Healthy controls consistently exhibited a greater magnitude of coherence in the synergistic AD-MD muscle pair in θ, α, β, and γ bands compared to all severities of stroke impairment investigated in this study. When comparing the various levels of stroke impairment, the non-synergistic BRD-MD muscle pair repeatedly showed that greater severity of stroke impairment coincides with higher magnitude of coherence in that connection in the lower δ and θ bands. Statistical tests on normalized coherence between healthy controls and chronic severe stroke patients also coincide with previous results from *Kisiel-Sajewicz et al.* in that significant difference in coherence was identified between deltoid and triceps muscles. *Kisiel-Sajewicz et al.* found significantly higher coherence for the aforementioned muscles in the $0 - 11$ Hz spectral range. The statistical tests from this study indicate significantly higher θ band

(4 – 8 Hz) coherence in healthy controls versus chronic severe patients in the TRIlat-MD muscle connection (p = 0.0315) as well as significantly higher α band (8 – 12 Hz) coherence in the TRIlong-PD muscle connection (p = 0.0018). An interesting observation to gather from the multiple-comparisons tests of coherence between stroke impairment levels is that higher magnitude of coherence in the synergistic coupling of AD and MD muscles is still associated with reduced stroke impairment severity. This significant difference in coherence between moderate and severe impairment stroke patients coincides with the more obvious observation found when comparing healthy controls to stroke patients in general. It is possible that functional coupling of synergistic muscles may prove to be a reliable biomarker in stroke motor recovery and assessment.

Both power spectral density and intermuscular coherence indicate some significance in the coupling of synergistic deltoid and triceps muscles when comparing neurologically healthy individuals and impaired stroke patients. These points are further solidified through the more complex muscle network analysis.

4.3 Fewer Muscle Networks Post-Stroke

It was identified that four muscle networks were necessary to explain coherence patterns in healthy controls but only three muscle networks were needed to explain coherence from the same task in moderate stroke survivors, and two muscle networks were identified for both moderate and severe stroke survivors. This is an interesting observation as the increased severity of stroke impairment is associated with reduced functional coupling in the upper arm muscles, indicating a simplified functional

control scheme. Another qualitative observation that can be gathered by the coherence patterns extracted by NNMF is that increased stroke impairment levels are associated with higher magnitude of coherence in the delta band. For example, the average peak coherence value for δ band extracted for the H1 network is approximately 0.2 whereas for the I1 network that value is just slightly higher than 0.2. However, the O1 network shows an increase from 0.2 to 0.3 for δ band coherence and finally the S1 network increases up to a magnitude of 0.6.

The topology of muscle network backbones identified by a minimum-spanning tree algorithm identified some key network edges that corroborated to previous muscle synergy findings. *Roh et al.* previously indicated the following synergistic muscles for the healthy controls: BRD-BIm, TRIlat-TRIlong, AD-MD, and MD-PD. The high strength network edges for healthy controls consisted of: BRD-BIm, TRIlat-TRIlong, AD-MD, and TRIlong-PD. The MD-PD synergistic pairs of muscles were identified as medium strength edges in half of the stable force generation healthy muscle networks. Mild stroke muscle networks involved AD-MD, MD-PD, and TRIlat-TRIlong as high strength edge weights that were also found to be synergistic muscles in Roh et al. (2015). The synergistic BRD-BIm muscle connection was not found to contribute much to either of the mild stroke muscle networks as they were found to be low strength edges. The coherence patterns associated with the I2 muscle network appears to include the combined α and β spectral ranges. Fractionation and merging of muscle synergies has previously been reported in motor-impairing disease studies and it is possible that the functional muscle connections in the alpha and beta bands merged

post-stroke due to the neurological consequences of stroke on the cortex and cortico-spinal pathways (Fisher et al., 2012). Moderate stroke networks included the following synergistic muscles during isometric force generation: BRD-BIm, TRIlat, TRIlong, AD-MD, AD-PD, and MD-PD. The coherence pattern associated with the O1 muscle network shows a merging of the δ, θ, and α bands whereas the β and γ bands are merged in the O2 network. Synergistic muscles from severe stroke patients during stable force generation involved: BRD-BIm, TRIlat-TRIlong, AD-MD, AD-PD, and MD-PD. TRIlat-TRIlong, BRD-BIm, and MD-PD were identified as high strength network edges during stable force generation whereas AD-MD and AD-PD were found to be considered medium strength edges in the muscle networks. Synergistic muscles co-activated in stable force generation are also confirmed to be functionally associated to each other in different frequency bands via intermuscular coherence.

It is evident that the functional motor control scheme is simplified post-stroke. Frequency bands are not segregated by separate muscle networks in stroke in contrast to healthy controls, especially higher frequency bands more commonly associated with sensorimotor tasks. The lower number of muscle networks in stroke patients suggests that not only muscle coordination but also the functional coupling between muscles is altered. Inducing the increase of coherence within these higher frequency bands may be key in successful motor rehabilitation post-stroke.

Roh et al., previously observed four muscle synergies needed to explain the sEMG activation patterns for both healthy and stroke groups, respectively. The stroke groups shared two similar synergies to the healthy control group but differed in abnormal co-

37

activation of deltoid head fibers. It is noteworthy that although the number of muscle synergies defined in the time domain were comparable across all four groups, the functional coupling of those synergies defined in the frequency domain is not the same. The apparent functional connectivity between AD and PD within stroke muscle networks coincides with the abnormal muscle synergy patterns identified by *Roh et al*.

According to *Kerkman et al.* it seems likely that intermuscular coherence at very low frequencies in the delta band identifies the covariation of rectified EMG envelopes that are crucial in muscle synergy analysis. Additionally, it was conjectured that muscle networks associated with higher intermuscular coherence content may in fact be isolating different functional pathways of the neuromuscular system (Kerkman et al., 2020). Indeed, synergistic muscles were identified to be high strength edges in coherence muscle networks with lower spectral components in the delta band for both healthy controls and all stroke impairment groups.

It is possible that cortical lesions caused by stroke impair the neural oscillatory drive to the upper-arm and elbow muscles in higher frequency bands by altering the corticospinal pathways, resulting in a simpler functional control scheme to compensate for lower efficiency in motor execution. The absence of unique coherence patterns in higher frequency bands in stroke patients is evidence of some alteration in the common input to motor neurons. Since functional connectivity seems to be highly affected by the anatomical muscle networks as suggested by *Kerkman et al.*, it is conceivable to reason that the alteration in muscle co-activation after stroke ultimately influences the magnitude and morphology of intermuscular coherence.

4.4 Study Limitations

This study has two limitations: only one trial was performed per target position and the isometric period of each trial was relatively short (3 – 6 s). To compensate for this, all trials per subject were concatenated to provide a greater number of samples for coherence analysis and a shorter windows size of 500 milliseconds was implemented for smoothing spectral features such as power spectral density and magnitude-squared coherence. Intermuscular coherence of stroke patients should be observed with a larger cohort and increased trial duration without inducing patient muscle fatigue or distress for the patients to validate the results of this study.

4.5 Future Work

Future work would benefit from combining brain networks, muscle networks, and muscle synergies to provide better insight on the negative effects of other motor-impairing diseases on the neuromuscular system and improve therapy and rehabilitation for those in need of it. Muscle networks have clinical monitoring potential and as such, the effects of motor rehabilitation in stroke patients on muscle network metrics should be determined as a potential biomarker of neurophysiological recovery.

CHAPTER 5 – CONCLUSION

Using novel muscle network analysis to assess the functional co-activation of muscles, it has been shown that post-stroke survivors exhibit differences in muscle connectivity during isometric force generation in upper arm reaching movements as compared to healthy controls in the frequency domain. Statistically significant reductions in power spectral density and intermuscular coherence were identified in higher frequency bands between healthy controls and stroke patients of mild, moderate, and severe impairment. Functional connectivity in eight key upper-arm muscles was assessed via intermuscular coherence and patterns in coherence were identified using non-negative matrix factorization. A reduced number of muscle networks was identified for increased severity of stroke impairment. Muscle networks were quantified with node strength. Synergistic muscles in stable force generation were found to be key network edges in muscle networks. Understanding the underlying neural drive to muscles in post-stroke survivors can prove vital in improving motor rehabilitation by identifying the abnormal nodes in the muscle networks and targeting them heavily in the guided physical therapy process.

CHAPTER 6 – SUPPLEMENTARY FIGURES

6.1 Additional Network Metric Figures

<center>(a)</center>

<center>(b)</center>
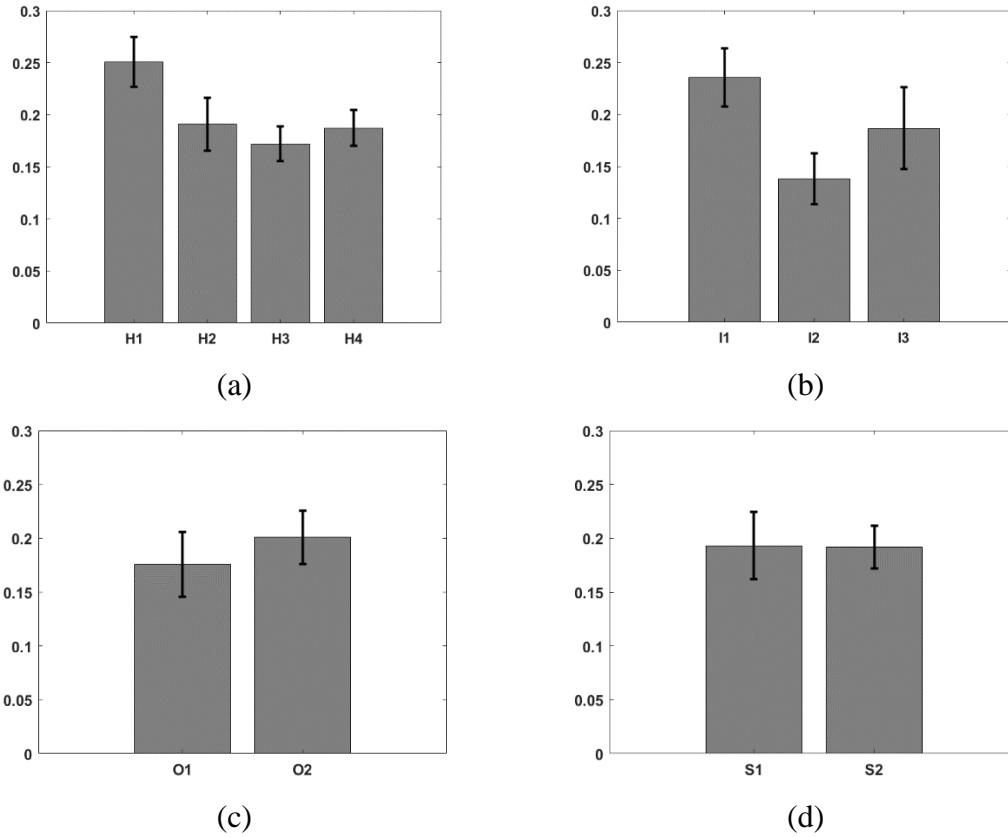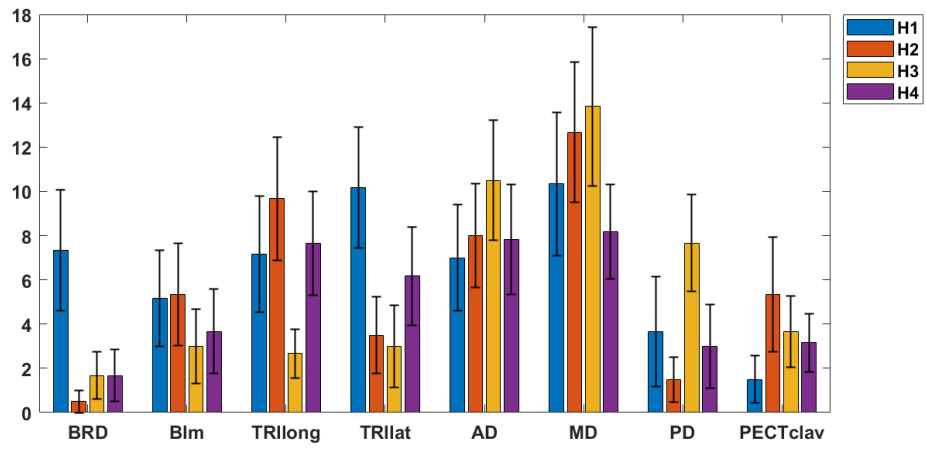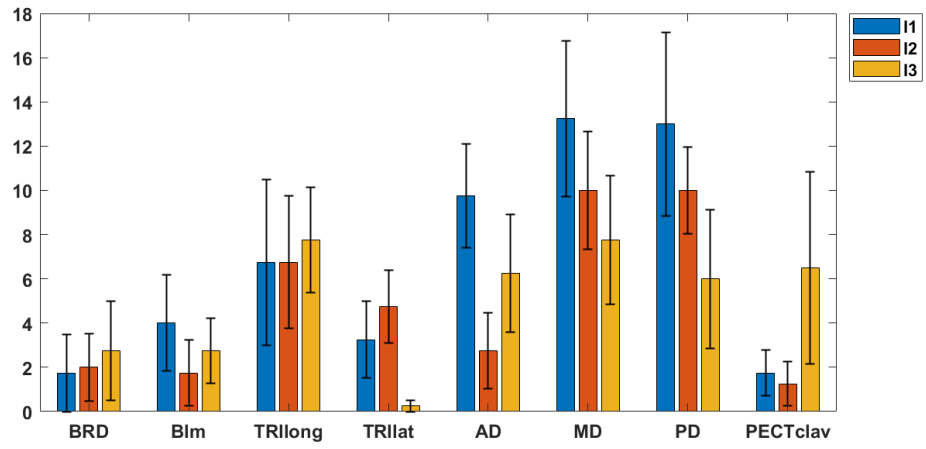
<center>(c)</center>
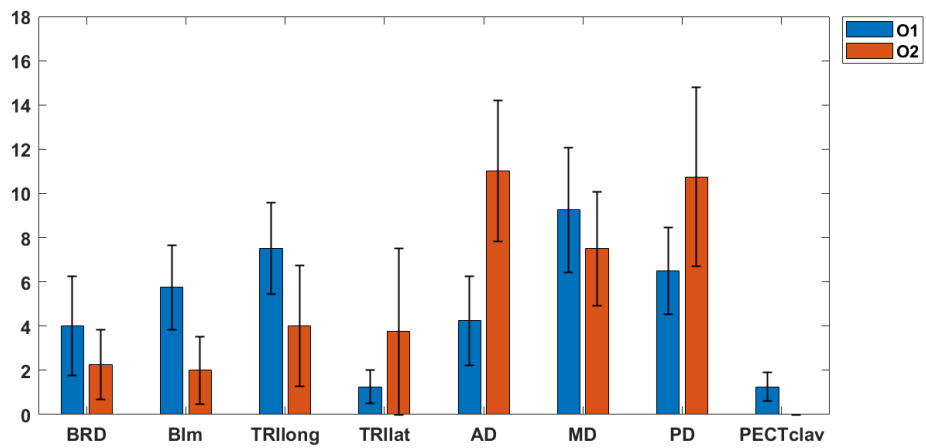
<center>(d)</center>

Figure 11. Global Efficiency Network Metric. (a) Healthy. (b) Mild Stroke. (c) Moderate Stroke. (d) Severe Stroke.
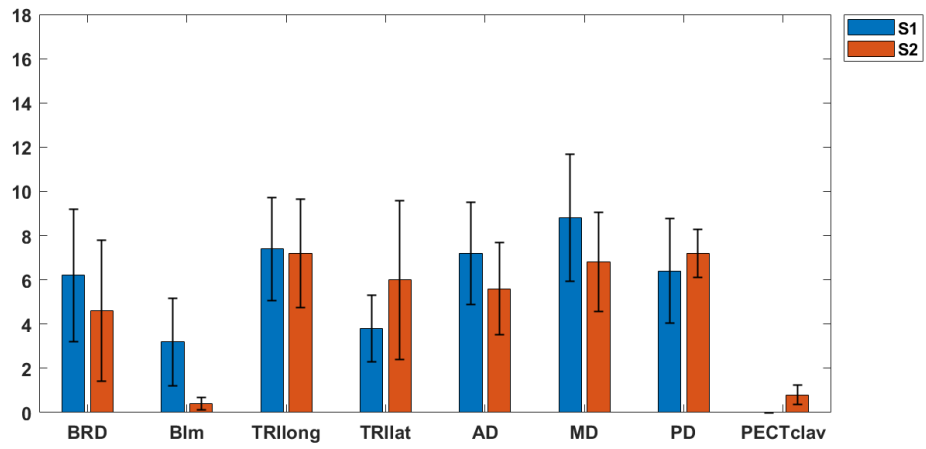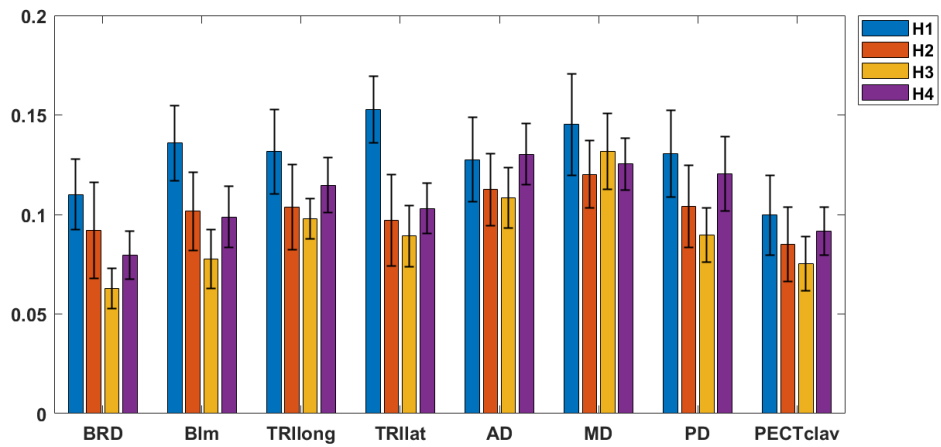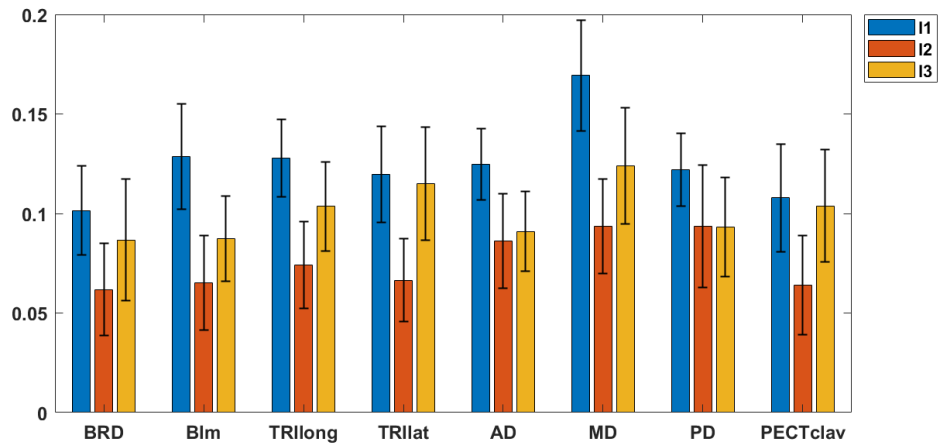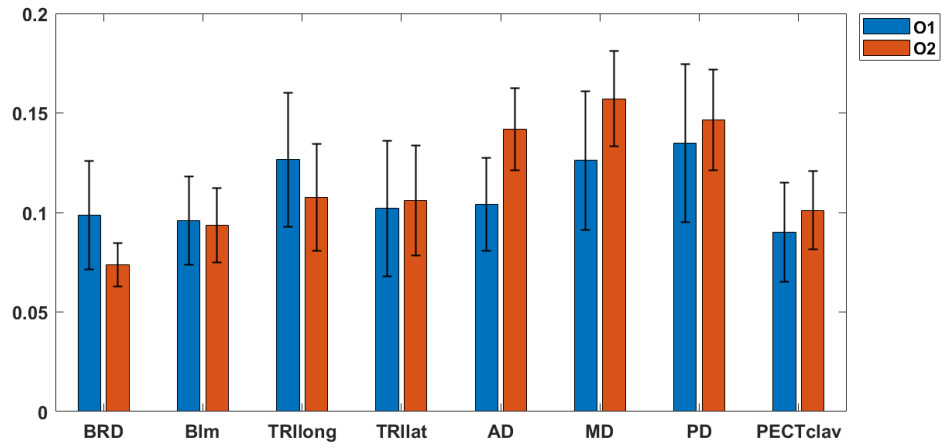
(a)

(b)

(c)

(d)

Figure 12. Betweenness Centrality Network Metric. (a) Healthy. (b) Mild Stroke. (c) Moderate Stroke. (d) Severe Stroke.
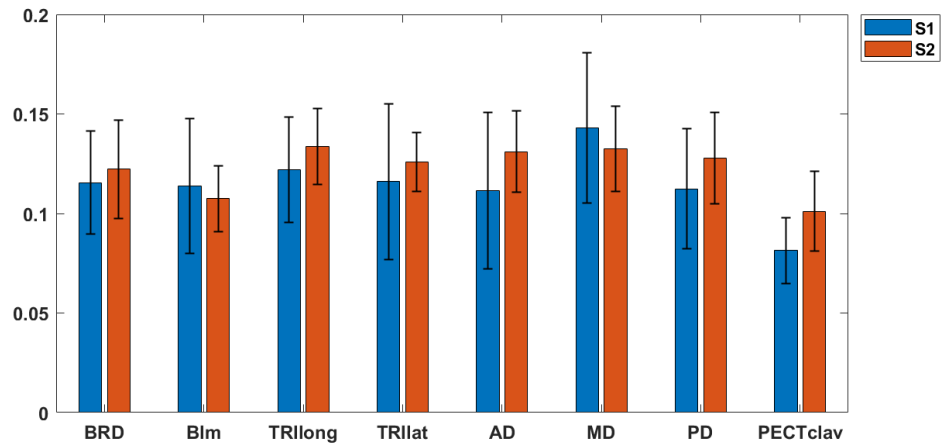

(a)

(b)

(c)

(d)

Figure 13. Clustering Coefficient Network Metric. (a) Healthy. (b) Mild Stroke. (c) Moderate Stroke. (d) Severe Stroke.

REFERENCES

[1]E. Bizzi, F. Mussa-Ivaldi, and S. Giszter, "Computations underlying the execution of movement: a biological perspective," Science, vol. 253, no. 5017, pp. 287–291, Jul. 1991.

[2]E. Bizzi, V. Cheung, A. Davella, P. Saltiel, and M. Tresch, "Combining modules for movement," Brain Research Reviews, vol. 57, no. 1, pp. 125–133, Jan. 2008.

[3]A. Davella, P. Saltiel, and E. Bizzi, "Combinations of muscle synergies in the construction of a natural motor behavior," Nature Neuroscience, vol. 6, no. 3, pp. 300–308, Feb. 2003.

[4]E. Bizzi and V. C. K. Cheung, "The neural origin of muscle synergies," Frontiers in Computational Neuroscience, vol. 7, Apr. 2013.

[5]D. D. Lee and H. S. Seung, "Learning the parts of objects by non-negative matrix factorization," Nature, vol. 401, no. 6755, pp. 788–791, Oct. 1999.

[6]X. Li, Y. Du, C. Yang, W. Qi, and P. Xie, "Merging of synergistic muscles and intermuscular coherence predict muscle coordination complexity," *2016 IEEE International Conference on Information and Automation (ICIA)*, 2016. p. 791-5.

[7]J. Roh, W. Z. Rymer, E. J. Perreault, S. B. Yoo, and R. F. Beer, "Alterations in upper limb muscle synergy structure in chronic stroke survivors," Journal of Neurophysiology, vol. 109, no. 3, pp. 768–781, Feb. 2013.

[8]J. Roh, W. Z. Rymer, and R. F. Beer, "Evidence for altered upper extremity muscle synergies in chronic stroke survivors with mild and moderate impairment," Frontiers in Human Neuroscience, vol. 9, no. 6, Nov. 2015.

[9] K. Kisiel-Sajewicz, Y. Fang, K. Hrovat, G. H. Yue, V. Siemionow, C.-K. Sun, A. Jaskólska, A. Jaskólski, V. Sahgal, and J. J. Daly, "Weakening of Synergist Muscle Coupling During Reaching Movement in Stroke Patients," Neurorehabilitation and Neural Repair, vol. 25, no. 4, pp. 359–368, Feb. 2011.

[10] K. M. Fisher, B. Zaaimi, T. L. Williams, S. N. Baker, and M. R. Baker, "B -band intermuscular coherence: a novel biomarker of upper motor neuron dysfunction in motor neuron disease," Brain, vol. 135, no. 9, pp. 2849–2864, Jun. 2012.

[11] C. M. Laine and F. J. Valero-Cuevas, "Intermuscular coherence reflects functional coordination," Journal of Neurophysiology, vol. 118, no. 3, pp. 1775–1783, Jan. 2017.

[12] H. B. Nguyen, S. W. Lee, M. L. Harris-Love, and P. S. Lum, "Neural coupling between homologous muscles during bimanual tasks: effects of visual and somatosensory feedback," Journal of Neurophysiology, vol. 117, no. 2, pp. 655–664, Jan. 2017.

[13] J. M. Kilner, S. N. Baker, S. Salenius, V. Jousmäki, R. Hari, and R. N. Lemon, "Task-dependent modulation of 15-30 Hz coherence between rectified EMGs from human hand and forearm muscles," The Journal of Physiology, vol. 516, no. 2, pp. 559–570, 1999.

[14] J. M. Kilner, S. N. Baker, S. Salenius, R. Hari, and R. N. Lemon, "Human Cortical Muscle Coherence Is Directly Related to Specific Motor Parameters," The Journal of Neuroscience, vol. 20, no. 23, pp. 8838–8845, Jan. 2000.

[15] T. W. Boonstra, A. Danna-Dos-Santos, H.-B. Xie, M. Roerdink, J. F. Stins, and M. Breakspear, "Muscle networks: Connectivity analysis of EMG activity during postural control," Scientific Reports, vol. 5, no. 1, Apr. 2015.

[16] J. N. Kerkman, A. Daffertshofer, L. L. Gollo, M. Breakspear, and T. W. Boonstra, "Network structure of the human musculoskeletal system shapes neural interactions on multiple time scales," Science Advances, vol. 4, no. 6, Jun. 2018.

[17] J. N. Kerkman, A. Bekius, T. W. Boonstra, A. Daffertshofer, and N. Dominici, "Muscle Synergies and Coherence Networks Reflect Different Modes of Coordination During Walking," *Frontiers in Physiology*, vol. 11, 2020.

[18] D. Mayhew, B. Bachrach, W.Z. Rymer, and R.F. Beer, "Development of the MAC ARM - a novel cable robot for upper limb neurorehabilitation," 9 International conference on Rehabilitation Robotics, pp. 209-302, 2005

[19] R. Beer, D. Mayhew, C. Bredfeldt, and B. Bachrach, "Technical evaluation of the MACARM: A cable robot for upper limb neurorehabilitation," 2008 2nd IEEE RAS & EMBS International Conference on Biomedical Robotics and Biomechatronics, 2008.

[20] L. Myers, M. Lowery, M. O'malley, C. Vaughan, C. Heneghan, A. S. C. Gibson, Y. Harley, and R. Sreenivasan, "Rectification and non-linear pre-processing of EMG signals for cortico-muscular analysis," *Journal of Neuroscience Methods*, vol. 124, no. 2, pp. 157–165, 2003.

[21] T. W. Boonstra and M. Breakspear, "Neural mechanisms of intermuscular coherence: implications for the rectification of surface electromyography," Journal of Neurophysiology, vol. 107, no. 3, pp. 796–807, Feb. 2012.

[22] T. Wojtara, F. Alnajjar, S. Shimoda, and H. Kimura, "Muscle synergy stability and human balance maintenance," Journal of NeuroEngineering and Rehabilitation, vol. 11, no. 1, p. 129, Aug. 2014.

[23] M. Rubinov and O. Sporns, "Complex network measures of brain connectivity: Uses and interpretations," *NeuroImage*, vol. 52, no. 3, pp. 1059–1069, Sep. 2010.

[24] Li, X., Shin, H., Zhou, P., Niu, X., Liu, J. and Rymer, W., 2014. Power spectral analysis of surface electromyography (EMG) at matched contraction levels of the first dorsal interosseous muscle in stroke survivors. *Clinical Neurophysiology*, 125(5), pp.988-994.